

Multiplicity-dependent saturation momentum in p -Pb collisions at 5.02 TeV

Takeshi Osada*

*Department of Natural Sciences, Faculty of Science and Engineering
Tokyo City University, Tamazutsumi 1-28-1, Setagaya-ku, Tokyo 158-8557, Japan
(Dated: November 9, 2021)*

Semi-inclusive transverse momentum spectra observed in proton-proton and proton-lead nuclear collisions at LHC energies obey a geometric scaling with a scaling variable using multiplicity-dependent saturation momentum. The saturation momentum extracted from the experimental data is proportional to the $1/6$ power of the hadron multiplicity in the final state. On the other hand, the system's transverse size is proportional to the $1/3$ power of the multiplicity, and the saturation momentum and the transverse size of the system are strongly correlated with the hadron multiplicity in the final state. Since the saturation momentum is proportional to the average transverse momentum of hadrons, one predicts average transverse momentum is also proportional to the $1/6$ power of the multiplicity, which is consistent with experimental results at the LHC energy. We found that a nuclear modification factor R_{pPb} calculated by the multiplicity-dependent saturation momentum decreases at $p_T \lesssim 1 \text{ GeV}/c$ and that our model can partially explain the R_{pPb} 's behavior thought to be caused by nuclear shadowing. On the other hand, Cronin enhancement experimentally observed at $2 \lesssim p_T \lesssim 6 \text{ GeV}/c$ is not reproduced. However, the experimental result, including the Cronin effect, can be reproduced well by introducing p_T dependence as a $4\sim 5\%$ correction to the multiplicity-dependent saturation momentum. We also discuss a relation between the geometric scaling in the semi-inclusive distributions and the string percolation model.

PACS numbers: 13.75.Cs, 24.60.Ky, 25.75.Gz

I. INTRODUCTION

The gluon saturation picture [1–4] has provided us with many hints for a unified understanding of multi-particle production in which strong interactions play a significant role. For example, in a Color Glass Condensate (CGC) model [5, 6] which is an effective theory to describe saturated gluons with small x , the saturation scale [7, 8] separates the classical gluon field into fast frozen color sources and slow dynamical color fields. The existence of the intrinsic scale of the transverse momentum $Q_s(x)$ is a crucial underlying assumption of the effective theory. Furthermore, by replacing p_T in a Bjorken x of the saturation scale $Q_s(x)$ with some constant characteristic one, we introduce the energy-dependent saturated momentum $Q_{\text{sat}}(W)$, which depends only on the collision energy W . Then, it is a unique scale that governs p_T spectra of the produced particles, and as a result, geometric scaling [9–11] (GS) emerges. The authors of Ref.[12–16] confirmed GS certainly holds for inclusive p_T spectra of high-energy pp , pA , and AA collisions.

In our previous work [17, 18], we confirmed that GS also holds even for semi-inclusive distributions. In these cases, we introduced a saturation momentum $Q_{\text{sat}}(W^*)$ that depends on the effective energy W^* , which has a one-to-one correspondence with the observed multiplicity in the final state instead of the initial colliding energy W . This paper will discuss based on a perspective that the physics of gluon saturation is a fundamental property and should serve as a comprehensive explanation of multi-

particle production at different reaction types, energies, and multiplicities.

Recently, a collective motion thought to be characteristic of the hadronic matter produced by the collisions of large systems such as AA has been found in high-multiplicity events by small systems such as pp and pA collisions [19, 20]. Therefore, another hint to the unified understanding of multi-particle production in any type of reaction would be seen the similarity in high multiplicity events of pp and pA collisions. The multiplicity dependence on the mean transverse momentum in pp , pA , and AA collisions is impressive because their dependence is significantly different for each reaction type, especially at high multiplicity [21]. In particular, theoretical studies need to explain a result that the multiplicity dependence on the mean transverse momentum of p -Pb collisions is weaker than that of pp for $dn/dy \gtrsim 20$.

The so-called cold nuclear matter effects observed in pA collisions has been investigated by experiments at RHIC [22–24] and LHC energies [25–27], and theoretical explanations have been added to those results [28–30]. An important observable, nuclear modification factor R_{pA} , is defined by a ratio of the p_T spectrum of pA collisions to that of pp collisions, with particular attention paid to the increase in the yield of p -Pb collisions known as the Cronin effect [31–33]. One considers the deviation of the value of R_{pA} from 1 as the nuclear matter effects on particle production, making it possible to investigate the multiple scattering effects in the nuclear medium including nuclear shadowing [34] and transverse momentum broadening [35]. One may also extract information on the small x gluon distribution of a nucleus in the early stage of collisions [36]. The CGC formalism has been successful in explaining these nuclear shadow-

* t-osada@tcu.ac.jp

ing, and transverse momentum broadening in pA collisions at the LHC [37]. For collisions of different system sizes, such as pA , two saturation momentum scales, i.e., Q_s^p for proton and Q_s^A for nucleus, are introduced into theoretical models. However, due to less constrained the initial value of those saturation scales, it gives theoretical uncertainties of the nuclear modification factor R_{pA} at LHC [38]. It has also been pointed out that fluctuations in protons' saturation momentum play a significant role in the multiplicity distribution of produced particles in pA collisions [39].

In this paper, the multiplicity-dependent saturation momentum is extracted using the geometric scaling property of the semi-inclusive p_T spectra in pp and p -Pb collisions. Furthermore, using the experimental results on the nuclear modification factor in the central rapidity region, we further investigate the saturation momentum that governs the multi-particle production process in p -Pb collisions.

This article is organized as follows. We briefly explain the geometric scaling for the semi-inclusive distribution and determine its parameters in Section II. Besides, by fitting a universal function of GS to the semi-inclusive p_T spectra observed in pp and p -Pb collisions at LHC energies, we determine the multiplicity-dependent saturation momentum $Q_{\text{sat}}(W^*)$ and the effective interaction radius R_T^* as a function of the multiplicity density in the central rapidity region. Then, we show that the experimental results on the multiplicity dependence of $\langle p_T \rangle$ are consistent with the GS's conjecture in Sec.III. In the Sec.IV, we clarify the role of the saturation momentum in the nuclear modification factor R_{pPb} by comparing our model calculations using $Q_{\text{sat}}(W^*)$ obtained for pp and p -Pb, respectively. We close with Sec.V containing the summary and some concluding remarks.

II. GS IN SEMI-INCLUSIVE TRANSVERSE MOMENTUM SPECTRA

Consider transverse momentum spectra of pp or p -Pb collisions with colliding (center of mass) energy W classified by the multiplicity of the charged hadrons in its final state. In the following formulation of our model, except for a determination part of the multiplicity-dependent saturation momentum and the universal functions, we follow the theoretical formulation developed in Ref. [17, 18] for pp collisions.

For each event multiplicity classes, the semi-inclusive transverse spectra of hadrons normalized by a effective crosssectional reaction area S_T^* can be scaled to an universal function

$$\frac{1}{S_T^*} \frac{1}{2\pi p_T} \frac{d^2 n_{\text{ch}}}{dp_T dy} = \mathcal{F}(\tau), \quad (1a)$$

with a scaling variable

$$\tau^{1/(2+\lambda)} \equiv \frac{p_T}{Q_{\text{sat}}(W^*)}, \quad (1b)$$

instead of the merely transverse momentum p_T . Here, $Q_{\text{sat}}(W^*)$ denotes a multiplicity-dependent saturation momentum as a function of the effective energy W^* [17, 18]. Equation (1a) is originally for the gluon p_T distribution based on the saturation picture [4, 7, 40]. We assume that the local parton-duality [41] holds in good approximation, and then hadron spectra observed have the same as a gluon distribution but different total multiplicity. The factor of the effective area S_T^* absorbs the ratio of the partons and hadrons' multiplicity as a constant. For an inclusive distribution, the saturation momentum (in literature, it is often referred to as an average saturation momentum or an energy-dependent saturation momentum)

$$Q_{\text{sat}}(W) = Q_0 \left(\frac{x_0 W}{Q_0} \right)^{\lambda/(\lambda+2)}, \quad (2)$$

is uniquely determined by collision energy W with constants $x_0 = 1.0 \times 10^{-3}$, $Q_0 = 1.0 \text{ GeV}/c$, $\lambda = 0.22$ [14, 42]. In our model [18], which deals with GS for the semi-inclusive spectrum, we determine W^* and S_T^* as fitting parameters to the semi-inclusive spectra for each multiplicity fixed by the event class. Therefore, $Q_{\text{sat}}(W^*)$ has a one-to-one correspondence with the multiplicity and regarded as a function of the multiplicity. Here, we assume that multiplicity-dependent saturation momentum $Q_{\text{sat}}(W^*)$ has the same energy dependence as that of Eq. (2), and it is a saturation momentum in which W in Eq. (2) is just replaced by W^* .

In our model, S_T^* and W^* are fitting parameters, which is equivalent to searching for S_T^* and $Q_{\text{sat}}(W^*)$ directly. In fact, there is the following relationship between W^* and Q_{sat} :

$$W^* = \frac{Q_{\text{sat}}}{x_0} \left(\frac{Q_{\text{sat}}}{Q_0} \right)^{2/\lambda}. \quad (3)$$

The function \mathcal{F} in Eq. (1a) is called universal function, and Tsallis type function is often used in GS [14]:

$$\mathcal{F}(\tau) = \left[1 + (q-1) \frac{\tau^{1/(2+\lambda)}}{\kappa} \right]^{-1/(q-1)}, \quad (4)$$

where q is a so-called non-extensive parameter and κ is a constant parameter which connects $Q_{\text{sat}}(W^*)$ as an intermediate energy scale and hadronization energy scale, freeze out temperature, for example. In previous analyses, we have determined $Q_{\text{sat}}(W^*)$ by assuming that a universal function for the inclusive spectra and that for the semi-inclusive spectra are the same. However, the p_T spectra broadens for the high multiplicity events at 7.0 and 13.0 TeV pp collisions. (This tendency already can be seen in Fig. 2 of [18].) Therefore, in this paper, we deal only with π^\pm spectra to exclude particles with large masses that may be sensitive in the large p_T region. One can also consider light hadrons such as pions to be more suitable for our assumption, such as the saturation picture of gluons and the subsequent particle production in the central rapidity.

TABLE I. Values of q and κ in the universal function Eq. (4) of geometrical scaling.

analysis	observable	q	κ	$\tau^{1/(2+\lambda)}$
pp incl [18]	charged	1.134	0.1292	< 40
pp incl	π^\pm	1.132	0.1111	< 2.5
pp incl	$\pi^\pm + K^\pm$	1.129	0.1211	< 2.5
pp, p -Pb semi-incl	π^\pm	1.145	0.1100	< 18

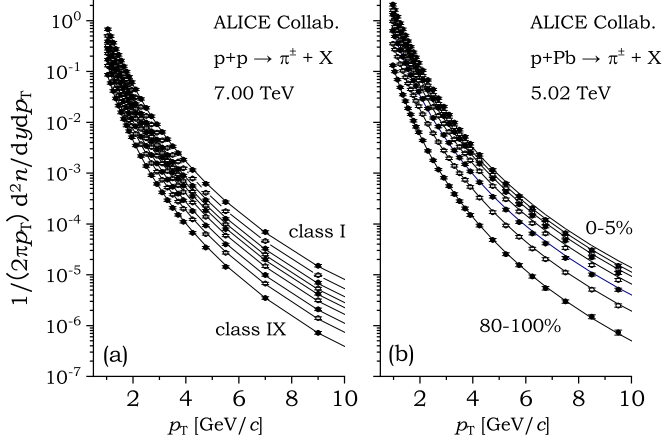


FIG. 1. Fit results of $S_T^* \mathcal{F}$ to the semi-inclusive spectra for (a) pp collisions at energy 7.00 TeV [43] (the multiplicity class is from I (top) to IX (bottom), and the class X is omitted because the multiplicity is too small). (b) The same as (a) but for p -Pb collisions at energy 5.02 TeV [44, 48] (the multiplicity class is from 0-5% (top) to 80-100% (bottom)). The value of $q = 1.145$ and $\kappa = 0.1100$ of the universal function \mathcal{F} of Eq. (4) is used. For the multiplicity of each class, the values of $Q_{\text{sat}}(W^*)$ and S_T^* are extracted from these fits.

Since the saturation picture can be universally applied to gluons inside highly relativistic contracted hadronic or nuclear matter, GS holds regardless of the collision system and it can be valid in high-energy pp and p -Pb collisions. Therefore, we search for $Q_{\text{sat}}(W^*)$ and S_T^* in addition to a universal function $\mathcal{F}(\tau)$ itself, which scales semi-inclusive distributions observed in pp and p -Pb collisions to the common universal function. In Fig. 1, we show two examples of the fit to the semi-inclusive spectra with $q = 1.145$, $\kappa = 0.1100$ for $p + p \rightarrow \pi^\pm + X$ at energy $W = 7.00$ TeV and for $p + \text{Pb} \rightarrow \pi^\pm + X$ at energy $W = 5.02$ TeV observed by ALICE Collaboration [43, 44]. Besides, Fig. 2 shows that 67 semi-inclusive distributions (947 data points), including the spectra shown in Fig. 1, observed in $\sqrt{s} = W = 2.76, 7.00, 13.0$ TeV pp collisions [43, 45, 46], and $W = 5.02$ TeV p -Pb collisions [44, 47, 48] almost perfectly scale to the universal function (1a) with $q = 1.145$ and $\kappa = 0.1100$. As shown in Fig. 2, we can find suitable $Q_{\text{sat}}(W^*)$ and an effective radius of the interaction area $R_T^* \equiv \sqrt{S_T^*/\pi}$ to scale the semi-inclusive p_T spectra of both pp and p -Pb col-

lisions to the same universal function $\mathcal{F}(\tau)$. Figs.3 (a) and 4 (a) shows $Q_{\text{sat}}(W^*)$ and R_T^* extracted from the semi-inclusive p_T spectra, respectively. Both $Q_{\text{sat}}(W^*)$ and R_T^* are functions of the multiplicity dn_π/dy of the final state pion in the central rapidity region. It should be noted that $Q_{\text{sat}}(W^*)$ and R_T^* are mutually correlated quantities because they are subject to the fixed multiplicity constraint of the semi-inclusive event as the following:

$$\frac{dn_\pi}{dy} = \frac{2\pi\kappa^2}{(2-q)(3-2q)} S_T^* Q_{\text{sat}}^2(W^*). \quad (5)$$

Considering that $R_T^* \propto [dn_\pi/dy]^{1/3}$ approximately holds as well known in the observation of the HBT effects [49–51], the saturation momentum should be proportional to the $1/6$ power of the multiplicity, $Q_{\text{sat}}(W^*) \propto [dn_\pi/dy]^{1/6}$. Actually, when $Q_{\text{sat}}(W^*)$ and R_T^* are plotted by $[dn_\pi/dy]^{1/6}$ and $[dn_\pi/dy]^{1/3}$, respectively, one confirms such dn/dy dependence as shown in Figs.3 (b) and 4 (b), which is consistent with the simple conjecture expected from GS.

We discuss somewhat peculiar multiplicity dependence on $Q_{\text{sat}}(W^*)$ extracted from p_T spectra of p -Pb collisions at 5.02 TeV observed by the ALICE Collaboration [44]. (See, Fig. 3 (a) and (b).) It is observed that the saturation momentum extracted from the spectra is significantly less multiplicity-dependent than the case of pp collisions. On the other hand, the extraction of $Q_{\text{sat}}(W^*)$ from spectra observed by CMS Collaboration [47] with the same collision system and the same energy gives almost the same results as that obtained in pp collisions. While ALICE Collaboration has published data on the transverse momentum spectra for $p_T < 20$ GeV/c, we used it for $0.6 < p_T < 3.0$ GeV/c to rule out hadron jet effects in the extraction of $Q_{\text{sat}}(W^*)$. Choosing the maximum $p_T = 2.0$ GeV/c, which is the same as the CMS, did not significantly affect results obtained. However, the rapidity range is slightly different between two collaborations, where CMS is $|y| < 1$, whereas ALICE is $0 < y < 0.5$, and ALICE has observed pions for the more central rapidity region. It is still unclear whether the rapidity window of the semi-inclusive p_T spectra affects the evaluation of $Q_{\text{sat}}(W^*)$ and R_T^* .

We fitted $Q_{\text{sat}}(W^*)$ and R_T^* shown in Figs. 3 (a) and Fig. 4 (a) by the following fitting formulae of $1/6$ and $1/3$ power of dn_π/dy , respectively;

$$Q_{\text{sat}}(W^*) = a_Q + b_Q \left(\frac{dn_\pi}{dy} \right)^{\frac{1}{6}}, \quad (6a)$$

$$R_T^* = a_R + b_R \left(\frac{dn_\pi}{dy} \right)^{\frac{1}{3}}. \quad (6b)$$

The values of the coefficients a_Q , b_Q , a_R and b_R fitted to the data of Figs.3 (a) and 4 (a) are shown in Table II. Here, if the constant terms a_Q and a_R can be ignored, the following relation is derived from Eq. (5);

$$\sqrt{\frac{(2-q)(3-2q)}{2\pi^2}} = \frac{\kappa b_Q b_R}{0.197 [\text{GeV}\cdot\text{fm}]}. \quad (7a)$$

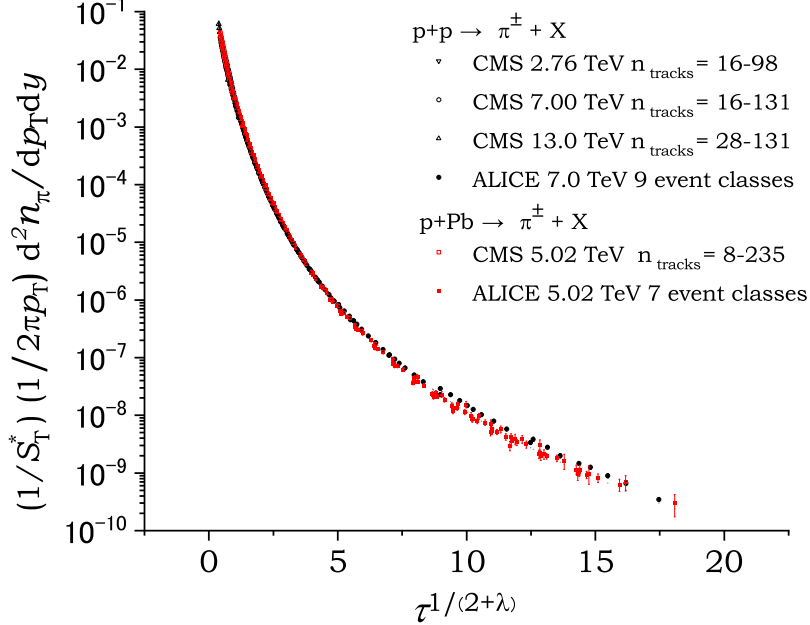


FIG. 2. Geometric scaling of the semi-inclusive p_T spectra in pp collisions (black symbols) for multiplicity class with track number $16 \leq n_{\text{tracks}} \leq 98$ at $\sqrt{s}=2.76$ TeV, $16 \leq n_{\text{tracks}} \leq 131$ at $\sqrt{s}=7.00$ TeV [45], and $28 \leq n_{\text{tracks}} \leq 172$ at $\sqrt{s}=13.0$ TeV [46] by CMS Collaboration (the pseudo rapidity window $|\eta| < 2.4$). The p_T spectra in pp collisions for 9 event classes with multiplicity range of $3.98 \leq dn_{\text{ch}}/dy \leq 20.1$ at 7.00 TeV [43] by ALICE Collaboration are also shown. For p -Pb collisions (red symbols) at 5.02 TeV for multiplicity class with track number $19 \leq n_{\text{tracks}} \leq 235$ by CMS [47] and ALICE Collaboration 7 event classes with multiplicity range of $4.4 \leq dn_{\text{ch}}/dy \leq 45$ [44, 48] are shown.

As shown in Table II, Eq. (7a) is approximately satisfied by the LHC energies of pp and p -Pb collisions. At the initial stage of collisions, gluon number density saturates due to their non-linear interactions. The inverse of saturation momentum $1/Q_{\text{sat}}$ gives a transverse cross-sectional size scale where saturated gluons are packed (one may consider it as a color flux tube size) [7, 17, 53]. If we evaluate the tube size scale from inclusive spectra, it is determined by solely the collision energy W and does not depend on the event multiplicity. For example, when the collision energy is $W = 7.0, 13.0$ TeV, the saturation momentum is $Q_{\text{sat}}(W) = 1.213$ and 1.289 GeV/ c , respectively. (These give flux tube size scale 0.162 and 0.153 fm, respectively.) However, the saturation momentum obtained from the semi-inclusive spectra is larger than that from the inclusive case especially in the high multiplicity event class. Therefore, it is considered that the size of the flux tube that appears in the initial stage of collision becomes smaller and shrinks slightly as the gluon multiplicity increases. As a result, the tube size appears as a multiplicity dependence such as $1/Q_{\text{sat}}(W^*) \propto [dn/dy]^{-1/6}$. On the other hand, since the reaction cross-sectional area S_T^* becomes large as $S_T^* \propto [dn/dy]^{2/3}$, one expects the number of flux tubes in the area S_T^* to be precisely proportional to dn/dy . In fact, Fig. 5 (b) shows that the number of color flux tubes

extracted from the pp and p -Pb semi-inclusive events increases linearly from $dn_\pi/dy \gtrsim 20$. Since the size of the color flux tube can be evaluated as $1/Q_{\text{sat}}$, we get the number of particles produced from a tube per unit rapidity as follows:

$$\frac{1}{n_{tb}} \frac{dn}{dy} \sim \frac{2\pi\kappa^2}{(2-q)(3-2q)} = \left[\frac{0.197[\text{GeV fm}]}{b_Q b_R} \right]^2, \quad (7b)$$

where $n_{tb} = S_T^* Q_{\text{sat}}^2(W^*)$ is the total number of color flux tubes packed in the effective reaction area. Based on the flux tube picture, the above equation near the central rapidity region does not depend on rapidity. The change in the slope of $Q_{\text{sat}}(W^*)$ and R_T^* in Fig. 3 and Fig. 4 observed by ALICE for p -Pb collisions at 5.02 TeV indicates that these b_Q and b_R changes. Therefore, it can be considered that the event multiplicity-dependence of both the flux tube size and the gluon interaction radius changes at $[dn/dy]^{1/6} \sim 1.6$. Before closing this section, let us analyze the transverse momentum spectrum obtained by the p -Pb collision [44] in two parts. One is the soft part, $0.5 \leq p_T \leq 1.5$ GeV/ c (soft π^\pm), and the other is the hard part, $3.0 \leq p_T \leq 19$ GeV/ c (hard π^\pm). By fitting data of each p_T window, the saturated momentum Q_{sat} can be extracted and compared to investigate the relationship with the effect of jet quenching [54]. (Since the measurement range of CMS Collabora-

TABLE II. The values of the parameters used in Eqs. (6a) and (6b) for fitting $Q_{\text{sat}}(W^*)$ and R_T^* extracted from the semi-inclusive p_T spectrum, respectively. We also show the right and left hand sides of Eq.(7a) to check the GS conjecture.

			$a_Q + b_Q(dn/dy)^{1/6}$		$a_R + b_R(dn/dy)^{1/3}$		eq.(7a)	
			a_Q	b_Q	a_R	b_R	l.h.s	r.h.s
$pp \rightarrow \pi^\pm + X$								
2.76 TeV[45]	$-1.0 < y < 1.0$		-0.019	0.854	0.006	0.371	0.175	0.177
7.00 TeV[45]	$-1.0 < y < 1.0$		-0.149	0.954	0.051	0.345	0.175	0.184
7.00 TeV[43]	$-0.5 < y < 0.5$		-0.225	0.985	0.073	0.345	0.175	0.190
13.0 TeV[46]	$-1.0 < y < 1.0$		-0.472	1.164	0.156	0.302	0.175	0.196
$pp \rightarrow h^\pm + X$								
5.02 TeV[52]	$-0.8 < \eta < 0.8$		-0.311	1.160	0.078	0.296	0.181	0.211
13.0 TeV[52]	$-0.8 < \eta < 0.8$		-0.390	1.323	0.072	0.246	0.181	0.200
$p\text{-Pb} \rightarrow \pi^\pm + X$								
5.02 TeV[47]	$-1.0 < y < 1.0$		0.078	0.899	0.030	0.358	0.175	0.180
5.02 TeV[44]	$0.0 < y < 0.5$		0.315	0.600	-0.130	0.446	0.175	0.149

tion is $p_T \leq 1.175$ GeV/c, it is classified as soft π^\pm , and the result is the same as a result shown in Fig.3 (b).) The multiplicity dependence of Q_{sat} obtained in these two p_T windows is shown in Fig.6. The multiplicity dependence of the saturation momentum obtained from soft π^\pm is not much different from results shown in Fig.3 (b) for low multiplicities. On the other hand, for high multiplicity, one observes that Q_{sat} is more clearly proportional to the 1/6 power of the multiplicity. For hard π^\pm , the multiplicity dependence is the same as the soft π^\pm case up to $[dn/dy]^{1/6} \sim 1.75$, but Q_{sat} is suppressed in a higher multiplicity. These results may indicate the formation of thin color flux tubes is suppressed by some reason in the initial state, or gluons (or pions) with high transverse momentum emitted from thin color flux tubes are suppressed due to interactions with hot hadronic matter or cold nuclear matter.

III. MEAN p_T IN SEMI-INCLUSIVE EVENTS

The different dn/dy dependence on the average transverse momentum $\langle p_T \rangle$ in pp and $p\text{-Pb}$ collisions has been reported in Ref. [21]. In GS model, since the average transverse momentum of the charged hadrons is proportional to the multiplicity-dependent saturation momentum $Q_{\text{sat}}(W^*)$, one expects $\langle p_T \rangle$ also proportional to the 1/6 power of the multiplicity fixed for the semi-inclusive events [17, 18]:

$$\langle p_T \rangle = \frac{2\kappa Q_{\text{sat}}(W^*)}{4-3q} \propto \left(\frac{dn}{dy} \right)^{1/6}. \quad (8)$$

Experimental data on the mean transverse momentum of π^\pm observed by CMS and the mean transverse momentum of charged hadron h^\pm observed by ALICE are re-plotted in Fig. 7 as a function of dn/dy to the 1/6 power. As shown in Fig. 7, the experimental results are substantially proportional to the multiplicity to

the 1/6 power. It is worth noting that the multiplicity dependence of $\langle p_T \rangle$ for $p\text{-Pb}$ data observed by the two experimental groups shows similar changes around $[dn/dy]^{1/6} \sim 1.6$ ($dn/dy \sim 20$), although the absolute value of it differs due to the difference in acceptance of the measurement. These experimental facts suggest that the multiplicity dependence of $Q_{\text{sat}}(W^*)$ changes at $dn/dy \sim 20$ in central rapidity region. Here, ignoring the contribution from a_Q and a_R in Eq. (6) as small and using Eqs. (7a) and (8), we obtain the following for the slope of the graph shown in Fig. 7;

$$\begin{aligned} \frac{\langle p_T \rangle}{[dn/dy]^{1/6}} &= \frac{0.197 [\text{GeV}\cdot\text{fm}]}{b_R} \frac{\sqrt{2(2-q)(3q-2)}}{\pi(4-3q)} \\ &= \frac{2\kappa b_Q}{4-3q} \approx 0.3 \sim 0.4 [\text{GeV}/c]. \end{aligned} \quad (9)$$

The multiplicity dependence of $\langle p_T \rangle$ given by Eq. (9) well explain the behavior of the experimental results. Moreover, one may explain the behavior of $\langle p_T \rangle$ for $p\text{-Pb}$ collisions observed by ALICE Collaboration for $[dn/dy]^{1/6} \gtrsim 1.6$ is due to the change of behavior of the $Q_{\text{sat}}(W^*)$. Namely, the decrease of b_Q and the increase of b_R (See, Table II) change the slope of $\langle p_T \rangle$ vs. $[dn/dy]^{1/6}$. Note that there is no change in the dependence proportional to the multiplicity's 1/6 power, just a change in the coefficients. As pointed out in Sec.II, the saturation momentum $Q_{\text{sat}}(W^*)$ extracted from the semi-inclusive p_T spectra in $p\text{-Pb}$ collisions changes its slope at $[dn/dy]^{1/6} \gtrsim 1.6$ (See, Fig. 3 (b)). Interestingly, both $Q_{\text{sat}}(W^*)$ and $\langle p_T \rangle$ show a qualitative change around the almost same dn/dy in their multiplicity dependence. Thus, the saturation momentum that governs the p_T spectra increases in proportion to the 1/6 power of multiplicity with the same proportional coefficient for low multiplicity events in both pp and $p\text{-Pb}$ collisions. However, for high multiplicity events in $p\text{-Pb}$ collisions, b_Q extracted from the ALICE data changes its value at

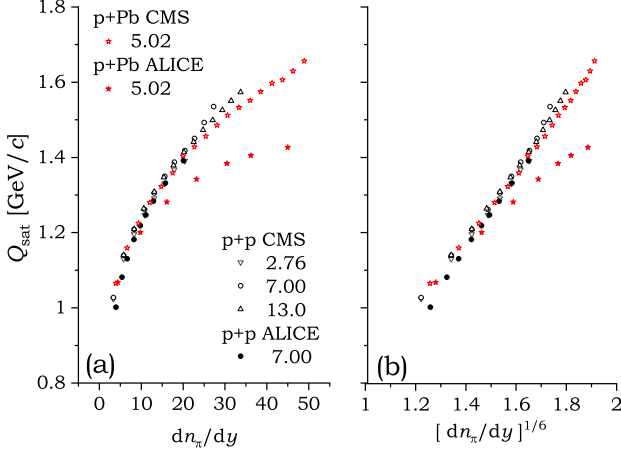


FIG. 3. (a) The multiplicity-dependent saturation momentum $Q_{\text{sat}}(W^*)$ obtained by the fitting Eq. (1) to the semi-inclusive π^\pm transverse spectra as a function of dn_π/dy . (b) The same as (a) but as a function of $[dn_\pi/dy]^{1/6}$.

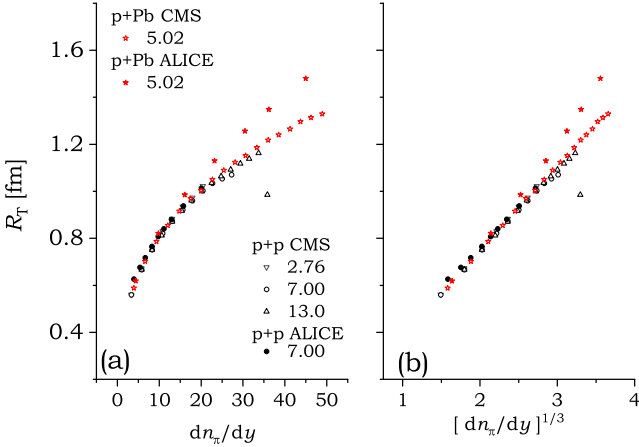


FIG. 4. (a) Effective transverse radii R_T^* of interaction cross sectional area obtained by the fitting Eq. (1) to the semi-inclusive π^\pm transverse spectra as a function of dn_π/dy . (b) The same as (a) but as a function of $[dn_\pi/dy]^{1/3}$.

$[dn/dy]^{1/6} \approx 1.6$. Furthermore, as can be seen from Fig. 4, the coefficient of $[dn/dy]^{1/3}$ for R_T^* also changes at the same multiplicity as $Q_{\text{sat}}(W^*)$. This is precisely what Eq. (9) expresses. On the other hand, for pp collisions, there are no indications that the multiplicity dependence of $\langle p_T \rangle$ changes up to the maximum multiplicity observed.

This multiplicity dependence change in $\langle p_T \rangle$ may be interpreted as follows. As can be seen from Fig. 5 (b), the number of flux tubes is proportional to the event multiplicity regardless of the reaction and energy. (Approximately four pions are produced per unit rapidity from one tube.) In the case of pp , the multiplicity increases as the tube's diameter decrease simultaneously as the sys-

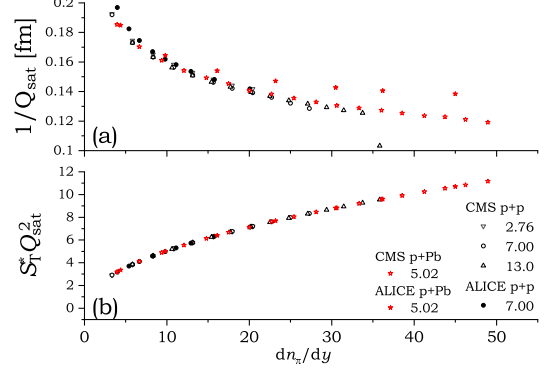


FIG. 5. dn/dy dependence of (a) $1/Q_{\text{sat}}(W^*)$ which can be interpreted as a scale of the radius of color flux tube and (b) $S_T^*Q_{\text{sat}}^2(W^*)$ which is the total number of the tubes produced in the interaction area.

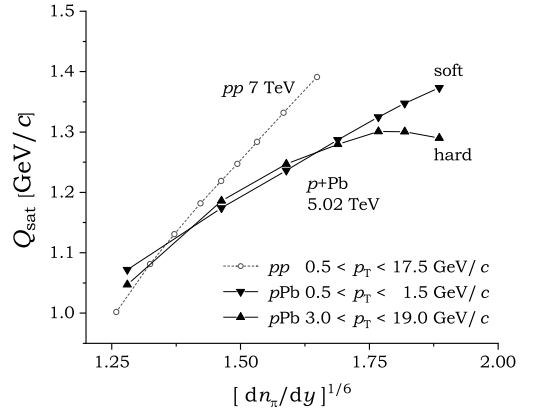


FIG. 6. The multiplicity dependence of the saturation momentum Q_{sat} obtained by fitting Eq. (1) to the semi-inclusive transverse momentum distribution in p -Pb collisions for soft p_T part ($0.5 \leq p_T \leq 1.5$ GeV/c) and hard p_T part ($3.0 \leq p_T \leq 19$ GeV/c). For reference purposes, we also show saturation momentum Q_{sat} obtained from pp collisions at 7.0 TeV.

tem's reaction size increases. (more tubes are packed in the interaction area.) In p -Pb, the multiplicity is increased by the same mechanism as the pp collision when the multiplicity is small. However, at a certain multiplicity, the flux tube's size becomes difficult to become thin, and instead, the reaction region becomes large, so that the multiplicity increases.

IV. NUCLEAR MODIFICATION FACTOR

In this paper, to introduce the multiplicity dependence of the saturation momentum, the originally existing p_T dependence of the saturation momentum has been

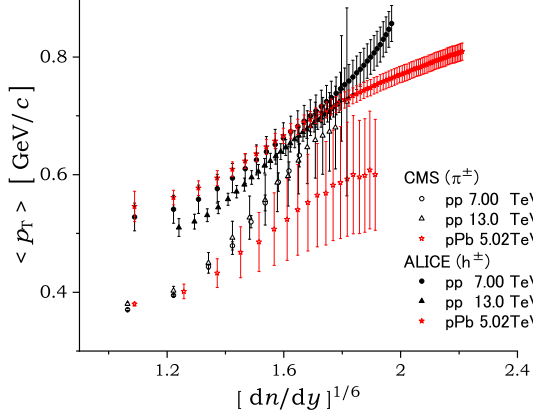


FIG. 7. Mean transverse momentum $\langle p_T \rangle$ of a charged hadron or charged pion as a function of $1/6$ power of dn/dy . The data on the multiplicity dn/dy dependence of $\langle p_T \rangle$ of charged hadrons observed by ALICE Collab.[21, 52], and the data on charged pions observed by CMS Collab.[45–47]

neglected by replacing it with a representative p_T , i.e., $Q_{\text{sat}}(W^*)$. If the nuclear modification factor does not include any final-state interactions, it may be the observable where the transverse momentum dependence, which we have been ignoring, is most pronounced. Therefore, we evaluate how much transverse momentum dependence is required for the obtained saturated momentum as a correction by comparing it with the available experimental data [55].

We have confirmed in Sec.II that the semi-inclusive p_T spectra of both pp and p -Pb scale to the same universal function. The saturation momentum, which plays a central role in the GS, behaves differently from pp , especially in high-multiplicity events of p -Pb collisions. In the case of p -Pb collisions, nuclear matter may affect the multiplicity-dependent saturation momentum. To investigate the nuclear matter effects on the saturation momentum in p -Pb collisions, the nuclear modification factor experimentally observed is compared with the model calculations. The modification factor is a ratio of p_T differential yield relative to the pp reference and it is defined by [48]

$$R_{\text{pPb}}^{\text{exp}}(p_T) = \frac{d^2 N_{\pi}^{\text{pPb}}/d\eta dp_T}{\langle T_{\text{pPb}} \rangle d^2 \sigma_{\text{ch}}^{\text{pp}}/d\eta dp_T}, \quad (10a)$$

where $\langle T_{\text{pPb}} \rangle = 0.0983 \text{ mb}^{-1}$ [48] is an average nuclear overlap function. In experiments, $R_{\text{pPb}}^{\text{exp}}$ is defined by the inclusive spectra, but we substitute it with the following equation using the semi-inclusive spectra to clarify a role of the saturation momentum:

$$R_{\text{pPb}}(p_T) = \frac{d^2 n_{\pi}^{\text{pPb}}/dy dp_T}{C d^2 n_{\text{ch}}^{\text{pp}}/dy dp_T}. \quad (10b)$$

Here, C in Eq. (10b) is a constant factor and is related to the experimental data of $\langle T_{\text{pPb}} \rangle$ and the total inelastic nucleon-nucleon cross section $\sigma_{\text{INEL}}^{\text{NN}} = 67.6 \text{ mb}$ [56] as follows:

$$C = \langle T_{\text{pPb}} \rangle \sigma_{\text{INEL}}^{\text{NN}} = 6.645. \quad (11)$$

We apply the multiplicity of semi-inclusive events for pp and p -Pb collisions as those of the average multiplicity of inclusive events, respectively: i.e., $\langle \frac{dN_{\pi}^{\text{pPb}}}{d\eta} \rangle \approx \frac{dn_{\pi}^{\text{pPb}}}{dy} = 16.81$ [57] and $\langle \frac{dN_{\pi}^{\text{pp}}}{d\eta} \rangle \approx \frac{dn_{\pi}^{\text{pp}}}{dy} = 4.13$ [56]. Therefore, by Eq. (6a) with values appearing in Table II, we have

$$Q_{\text{sat}}^{\text{pp}}(W^*) = 1.158 \text{ GeV}/c, \quad (12a)$$

$$Q_{\text{sat}}^{\text{pPb}}(W^*) = 1.276 \text{ GeV}/c. \quad (12b)$$

The nuclear modification factor R_{pPb} calculated by Eqs. (12a) and (12b) for the multiplicity-dependent saturation momentum of pp and p -Pb collisions, respectively, is shown by the broken line in FIG.8(a). We can partially reproduce R_{pPb} , such as suppression in the low p_T region and asymptotic behavior in the high p_T region. However, the simple calculation using Eqs. (12a) and (12b) overestimates R_{pPb} in the low p_T region compared to the experimental data and cannot reproduce the so-called Cronin enhancement.

Let us introduce p_T dependence as a phenomenological side effect on the saturation momentum $Q_{\text{sat}}(W^*)$, which has been regarded as a function of effective energy W^* (or average multiplicity dn/dy) only. Recall that the saturation momentum $Q_{\text{sat}}(W)$ is derived from an intermediate energy scale $Q_s^2(x) \equiv Q_0^2(x_0/x)^\lambda$ given by Bjorken $x = p_T/W$. Then Q_{sat} is defined with the solution p_T satisfying $p_T = Q_s^2(p_T/W)$. Therefore, this is a good approximation for $p_T \sim Q_{\text{sat}}$ and neglects the weak p_T dependence in $p_T \gg Q_{\text{sat}}$ and $p_T \ll Q_{\text{sat}}$ region, resulting in deviations from the original intermediate energy scale $Q_s(x)$ (See Fig. 1 in Ref. [18]). This weak p_T dependence may need to be taken into account, especially for observables such as Eq. (10b), which is sensitive to the behavior of p_T . Another reason to introduce this effect is to investigate the unknown detail of gluon recombination effect in multi-particle production from experimental data. (Of course, it is not possible to distinguish whether recombination occurred before or after the color flux tube formation.) We introduce such an effect phenomenologically and investigate whether it contributes to explaining $R_{\text{pPb}}^{\text{exp}}$ obtained in the experiment [48]. Thus, instead of Eq. (12b), we introduce modification for $Q_{\text{sat}}^{\text{pPb}}(W^*)$ given by Eq. (12c) as the following;

$$Q_{\text{sat}}^{\text{pPb}}(W^*) = a_Q + b_Q \left[\frac{dn_{\pi}^{\text{pPb}}}{dy} + \delta \right]^{1/6}, \quad (12c)$$

where

$$\delta = \alpha \left(\frac{p_T - \beta Q_{\text{sat}}^{\text{pp}}}{Q_{\text{sat}}^{\text{pp}}} \right) \exp \left[\frac{-p_T}{\gamma Q_{\text{sat}}^{\text{pp}}} \right]. \quad (12d)$$

TABLE III. The values of the parameters used in Eq. (12d) giving $R_{p\text{Pb}}(p_T)$ (solid curve) in Fig. 8.

dn_{π}^{pPb}/dy	$dn_{\text{ch}}^{\text{pp}}/d\eta$	α	β	γ	χ^2/dof
16.8	4.13	6.05	0.886	1.56	1.13/46

We show the results of fitting of Eq. (10b) with Eq. (11) and (12) to the experimental data $R_{p\text{Pb}}^{\text{exp}}(p_T)$ by the solid line in Fig. 8 (a), and the values of the parameters of Eq. (12d) in Table III. As shown in Fig. 8 (b), one can well reproduce the experimental data of the nuclear modification factor within 4% change for saturation momentum $p_T \lesssim 20$ GeV/c. In particular, the Cronin effect, in which an enhancement peak appears around $p_T = 2 \sim 6$ GeV/c in $R_{p\text{Pb}}^{\text{exp}}$, is explained by being about 1% larger than the multiplicity-dependent saturation momentum of p -Pb, Eq. (12b). Note that the original saturation scale $Q_s(x)$ with fixed collision energy W depends on the power of the gluon's transverse momentum; $Q_s(x) \propto p_T^{-\lambda/2}$. For example, when comparing the value of the saturation scale at $p_T \approx 1$ GeV/c and 5 GeV/c, the value at 5 GeV/c is about 15% smaller than the value at $p_T \approx 1$ GeV/c. Hence, the direction of the correction that reintroduces the weak p_T dependence of $Q_s(x)$ is the opposite direction of the correction required to explain the experimental result of $R_{p\text{Pb}}^{\text{exp}}$.

There are two possibilities to explain this variation in the saturation momentum $Q_{\text{sat}}(W^*)$. One possibility is that the p_T dependence in saturation momentum may be explained as the effects of interactions such as absorption and emission of gluons after flux tubes decay. The other is that such fluctuation may have already existed around the average saturation momentum at the time the color flux tube was formed. The former suggests that the application of parton-hadron duality requires caution. It may be possible to study these two possibilities by similar analyzing a nuclear modification factor by using prompt photons [58] in the same way as discussed in this article.

V. SUMMARY AND CONCLUDING REMARKS

Semi-inclusive spectra of pp and p -Pb collisions normalized by the $1/3$ power of the multiplicity scales to the same universal function using a saturation momentum proportional to the $1/6$ power of the multiplicity. The agreement between the experimental results and GS conjecture suggests that the saturation momentum, determined by a multiplicity of the final state (by assuming local parton hadron duality, it also depends on the gluon's initial state) dominates the multi-particle production regardless of the reaction type and collision energy. The existence of geometric scaling across different reactions such as proton-proton and proton-nucleus collisions strongly suggests the gluon saturation mechanism in the early stage of the reaction, which should be

a physics common to the elementary processes of phenomena on the multi-particle production. One of the advantages of GS analysis is that one can derive information on color flux tube formation in the early stage of hadronic or nuclear collisions from the multiplicity dependent saturation momentum $Q_{\text{sat}}(W^*)$. The information may be carried by the coefficients b_Q and b_R in Eqs. (6a) and (6b). Moreover, there is a constraint condition between them as Eqs. (7) or (9). Based on a color flux tube picture with these equations, we pointed out a reason why the multiplicity dependence of mean transverse momentum at high multiplicity in p -Pb collisions varies compared to pp collisions is a change of the multiplicity dependence of the diameter of the color flux tube and the size of the area packed tubes. Furthermore, observations of the nuclear modification factor may suggest that the multiplicity-dependent saturation momentum needs to introduce small transverse momentum dependence. However, the physical origin of this correction for the multiplicity-dependent saturation momentum is still unclear.

The string percolation model [59–62] has clear correspondence with the geometric scaling [63] examined in detail in this paper. Before closing this last section, let us consider why the multiplicity dependence of saturation momentum differs between pp and p -Pb collisions using the string percolation model. Consider a color string produced in a region S_T in pp or p -Pb collisions; given the cross-sectional area $\sigma_1 = \pi r_0^2$ of one string and the string density $\eta = N\sigma_1/S_T$ in the area S_T , we have the average number of effective strings $\langle N \rangle$ as the following, (See, Appendix A);

$$\langle N \rangle = S_T \frac{(1 - e^{-\eta})}{\pi r_0^2 F(\eta)}, \quad (13)$$

where $F(\eta)$ is a color reduction factor

$$F(\eta) = \sqrt{\frac{1 - e^{-\eta}}{\eta}}. \quad (14)$$

By noting that $\langle N \rangle \approx S_T Q_{\text{sat}}$, the corresponding saturation momentum is given by

$$Q_{\text{sat}}^2 \propto \begin{cases} \sqrt{\eta} & \text{for } \eta \gg 1, \\ \eta & \text{for } \eta \ll 1. \end{cases} \quad (15)$$

It is also interesting to note that if S_T is proportional to the $2/3$ power of multiplicity, $\sqrt{\eta}$ (for the case of high multiplicity case) is proportional to the $1/6$ power of multiplicity, which is consistent with the conclusion reached in this paper.

In the string percolation model, the multiplicity dependence of the saturation momentum (the dependence of the inverse of the effective string radius) is explained as a function of the string density. Therefore, the obtained results that the multiplicity dependence of the saturated momentum in pp and p -Pb is different for high multiplicity events suggest that the string densities are

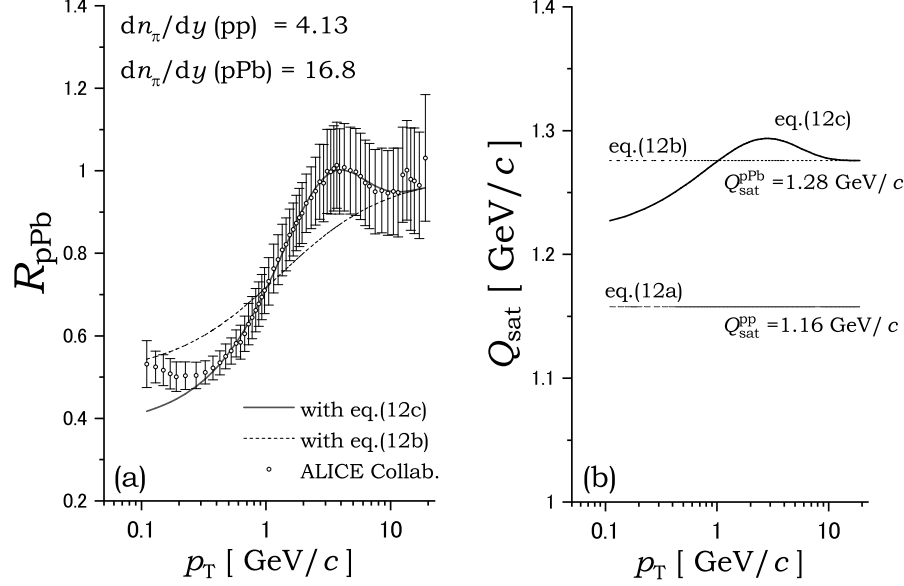


FIG. 8. (a) Comparison of the nuclear modification factor (10b) with ALICE data for p -Pb collision at 5.02TeV by saturation momentum with Eq(12b) and (12c) shown in the right panel (b).

substantially different in pp and p -Pb when the multiplicity is sufficiently large. Our result that the multiplicity dependence of saturated momentum is different for pp and p -Pb, and smaller for p -Pb compared to pp , suggests that the color overlap is larger for p -Pb than for pp when comparing events of the same multiplicity. It can also be understood that the transverse reaction area S_T with the same multiplicity as pp is larger for p -Pb, since the multiplicity decreases as the string overlap increases.

The suggestion that there are more overlapping strings in p -Pb than in pp may be naturally attributed to the effect of nucleons existing around the reaction region that are not present in the case of pp . The color flux tubes (effective strings) that lead to the large multiplicity of final states may increase the string density by exciting (or some interactions with) the surrounding nuclear matter.

The next step in our work is to analyze the semi-inclusive p_T spectrum obtained from AA collisions to determine a multiplicity dependent saturation momentum. Furthermore, the multiplicity dependence of the mean transverse momentum of Pb-Pb collisions is even weaker than that of p -Pb [21]. We need to investigate whether multiplicity-dependent saturation momentum extracted from the AA collisions also satisfies the 1/6 power law of the multiplicity, and clarify the difference between p -A and AA from the viewpoint of a multiplicity-dependent saturation momentum. We plan to investigate those issues at some other opportunity.

ACKNOWLEDGMENTS

This work was supported by JSPS KAKENHI Grant Number 20K03978.

Appendix A: String percolation model

Suppose that after high-energy pp or p -Pb collisions, N strings are generated and packed into the cross-sectional area S . Furthermore, suppose the cross-sectional area of each string is given by $\sigma_1 = \pi r_0^2$, and the multiplicity generated from one string is μ_1 . When n strings overlap in an area S_n , the color fields in that area are must be summed up like a vector. Therefore, the multiplicity of hadrons generated from the overlapped n strings is not proportional to n but to \sqrt{n} . Therefore, as the density of the strings increases, the multiplicity decreases. Then, the multiplicity produced in the region $S = \sum_n S_n$ is as follows [62]

$$\mu = \sum_{n=1}^N \frac{\sqrt{n} S_n}{\sigma_1} \mu_1. \quad (\text{A1})$$

On the other hand, the mean square transverse momentum must be summed like a scalar:

$$\langle p_T^2 \rangle = \frac{N \mu_1}{\mu} \langle p_T^2 \rangle_1 = \frac{N \langle p_T^2 \rangle_1}{\sum_{n=1}^N \sqrt{n} S_n / \sigma_1}. \quad (\text{A2})$$

In the limit of $N, S \rightarrow \infty$, assuming that the probability of finding the region of n strings form a cluster, $p(n) =$

S_n/S , obeys the Poisson distribution with the mean value

$$\eta \equiv N\sigma_1/S = \left(\frac{r_0^2}{R^2}\right) N, \quad (\text{A3})$$

the multiplicity of the final state is as follows:

$$\mu = \frac{S}{\sigma_1} \sum_{n=1}^{\infty} \frac{\sqrt{n} \eta^n}{n!} e^{-\eta} \mu_1. \quad (\text{A4})$$

Therefore, the color reduction factor $F(\eta)$, which is defined by the reduction rate of multiplicity due to the fusion of strings, is given by

$$F(\eta) \equiv \frac{\mu}{N\mu_1} = \frac{1}{\eta} \sum_{n=1}^{\infty} \sqrt{n} \frac{\eta^n e^{-\eta}}{n!} \approx \sqrt{\frac{1-e^{-\eta}}{\eta}}. \quad (\text{A5})$$

From Eq.(A2), we also get the mean squared transverse momentum as follows:

$$\langle p_T^2 \rangle = \frac{\langle p_T^2 \rangle_1}{F(\eta)}. \quad (\text{A6})$$

Note here that $\sigma_1 F(\eta)$ can be interpreted as the cross-sectional area of the effective string, which may be equivalent to the flux tubes in the Glasma picture, formed in

the color electric field. Hence, the area occupied by the stings $S - S_0$ divided by the area of the effective string $\sigma_1 F(\eta)$ gives the average number of effective strings (the average number of color tubes);

$$\langle N \rangle = \frac{S - S_0}{\sigma_1 F(\eta)} = \frac{R^2}{r_0^2} \frac{(1 - e^{-\eta})}{F(\eta)}. \quad (\text{A7})$$

Here, noting the correspondence between the effective string and the color flux tube in the Glass picture, we have

$$\langle N \rangle = \pi R^2 \frac{(1 - e^{-\eta})}{\pi r_0^2 F(\eta)} \rightarrow S_T Q_{\text{sat}}^2. \quad (\text{A8})$$

Thus the saturated momentum is related to the string mean density, and we also get

$$Q_{\text{sat}}^2 = \frac{\sqrt{\eta (1 - e^{-\eta})}}{\pi r_0^2}. \quad (\text{A9})$$

Hence, we confirmed from Eq. (A8) that the saturation momentum Q_{sat} certainly depends on the multiplicity of the final state hadrons through the string density η , and the behavior changes as follows depending on whether η is large or small:

$$Q_{\text{sat}}^2 \propto \begin{cases} \sqrt{\eta} & \text{for } \eta \gg 1, \\ \eta & \text{for } \eta \ll 1. \end{cases} \quad (\text{A10})$$

-
- [1] Y. V. Kovchegov and E. Levin, *Quantum chromodynamics at high energy*, Vol. 33 (Cambridge University Press, 2012) ISBN 9780521112574, 9780521112574, 9781139557689, <http://www.cambridge.org/de/knowledge/isbn/item6803159>
- [2] L. V. Gribov, E. M. Levin, and M. G. Ryskin, Phys. Rept. **100**, 1 (1983)
- [3] J. P. Blaizot and A. H. Mueller, Nucl. Phys. **B289**, 847 (1987)
- [4] D. Kharzeev and M. Nardi, Phys. Lett. **B507**, 121 (2001), arXiv:nucl-th/0012025 [nucl-th]
- [5] E. Iancu, A. Leonidov, and L. McLerran, in *QCD perspectives on hot and dense matter. Proceedings, NATO Advanced Study Institute, Summer School, Cargese, France, August 6-18, 2001* (2002) pp. 73-145, arXiv:hep-ph/0202270 [hep-ph]
- [6] J.-P. Blaizot and F. Gelis, *Quark gluon plasma. New discoveries at RHIC: A case of strongly interacting quark gluon plasma. Proceedings, RBRC Workshop, Brookhaven, Upton, USA, May 14-15, 2004*, Nucl. Phys. **A750**, 148 (2005), arXiv:hep-ph/0405305 [hep-ph]
- [7] D. Kharzeev and E. Levin, Phys. Lett. **B523**, 79 (2001), arXiv:nucl-th/0108006 [nucl-th]
- [8] F. Gelis, E. Iancu, J. Jalilian-Marian, and R. Venugopalan, Ann. Rev. Nucl. Part. Sci. **60**, 463 (2010), arXiv:1002.0333 [hep-ph]
- [9] A. M. Stasto, K. J. Golec-Biernat, and J. Kwiecinski, Phys. Rev. Lett. **86**, 596 (2001), arXiv:hep-ph/0007192 [hep-ph]
- [10] E. Iancu, K. Itakura, and L. McLerran, Nucl. Phys. **A708**, 327 (2002), arXiv:hep-ph/0203137 [hep-ph]
- [11] E. Iancu, K. Itakura, and L. McLerran, *Particles and nuclei. Proceedings, 16th International Conference, PANIC'02, Osaka, Japan, September 30-October 4, 2002*, Nucl. Phys. **A721**, 293 (2003)
- [12] M. Praszalowicz, Phys. Rev. Lett. **106**, 142002 (2011), arXiv:1101.0585 [hep-ph]
- [13] M. Praszalowicz, Phys. Lett. **B727**, 461 (2013), arXiv:1308.5911 [hep-ph]
- [14] L. McLerran and M. Praszalowicz, Phys. Lett. **B741**, 246 (2015), arXiv:1407.6687 [hep-ph]
- [15] M. Praszalowicz and A. Francuz, Phys. Rev. **D92**, 074036 (2015), arXiv:1507.08186 [hep-ph]
- [16] M. Praszalowicz, *Proceedings, International Meeting of Excited QCD 2015: Tatranska Lomnica, Slovakia, March 8-14, 2015*, Acta Phys. Polon. Supp. **8**, 399 (2015), arXiv:1505.02458 [hep-ph]
- [17] T. Osada and M. Ishihara, J. Phys. **G45**, 015104 (2018), arXiv:1702.07440 [hep-ph]
- [18] T. Osada and T. Kumaoka, Phys. Rev. **C100**, 034906 (2019), arXiv:1904.10823 [hep-ph]
- [19] R. Preghenella, in *17th International Conference on Strangeness in Quark Matter (SQM 2017) Utrecht, the Netherlands, July 10-15, 2017* (2018) arXiv:1804.03474 [hep-ex], <http://inspirehep.net/record/1667029/files/1804.03474.pdf>
- [20] V. Khachatryan *et al.* (CMS), Phys. Lett. **B765**, 193 (2017), arXiv:1606.06198 [nucl-ex]

- [21] B. B. Abelev *et al.* (ALICE), Phys. Lett. **B727**, 371 (2013), arXiv:1307.1094 [nucl-ex]
- [22] A. Adare *et al.* (PHENIX), Phys. Rev. C **88**, 024906 (2013), arXiv:1304.3410 [nucl-ex]
- [23] C. Aidala *et al.* (PHENIX), Phys. Rev. C **99**, 044912 (2019), arXiv:1809.09045 [hep-ex]
- [24] C. Aidala *et al.* (PHENIX), Phys. Rev. C **101**, 034910 (2020), arXiv:1906.09928 [hep-ex]
- [25] B. Abelev *et al.* (ALICE), Phys. Rev. Lett. **110**, 082302 (2013), arXiv:1210.4520 [nucl-ex]
- [26] J. Adam *et al.* (ALICE), Phys. Rev. C **91**, 064905 (2015), arXiv:1412.6828 [nucl-ex]
- [27] V. Khachatryan *et al.* (CMS), JHEP **04**, 039 (2017), arXiv:1611.01664 [nucl-ex]
- [28] A. Rezaeian and Z. Lu, Nucl. Phys. A **826**, 198 (2009), arXiv:0810.4942 [hep-ph]
- [29] A. H. Rezaeian, *Proceedings, Europhysics Conference on High energy physics (EPS-HEP 2009): Cracow, Poland, July 16-22, 2009*, PoS **EPS-HEP2009**, 045 (2009), arXiv:0909.2664 [hep-ph]
- [30] A. Dumitru, D. E. Kharzeev, E. M. Levin, and Y. Nara, Phys. Rev. C **85**, 044920 (2012), arXiv:1111.3031 [hep-ph]
- [31] J. Cronin, H. J. Frisch, M. Shochet, J. Boymond, R. Mermod, P. Piroue, and R. L. Sumner, Phys. Rev. D **11**, 3105 (1975)
- [32] D. Kharzeev, Y. V. Kovchegov, and K. Tuchin, Phys. Rev. **D68**, 094013 (2003), arXiv:hep-ph/0307037 [hep-ph]
- [33] E. Iancu, K. Itakura, and D. N. Triantafyllopoulos, Nucl. Phys. **A742**, 182 (2004), arXiv:hep-ph/0403103 [hep-ph]
- [34] M. Arneodo, Phys. Rept. **240**, 301 (1994)
- [35] A. Accardi(12 2002), arXiv:hep-ph/0212148
- [36] A. Dumitru, G. Kapilevich, and V. Skokov, Nucl. Phys. A **974**, 106 (2018), arXiv:1802.06111 [hep-ph]
- [37] J. Jalilian-Marian and A. H. Rezaeian, Phys. Rev. D **85**, 014017 (2012), arXiv:1110.2810 [hep-ph]
- [38] A. H. Rezaeian, Phys. Lett. **B718**, 1058 (2013), arXiv:1210.2385 [hep-ph]
- [39] L. McLerran and M. Praszalowicz, Annals Phys. **372**, 215 (2016), arXiv:1507.05976 [hep-ph]
- [40] L. McLerran, *High energy strong interactions. Proceedings, International Symposium, HESI10, Kyoto, Japan, August 9-13, 2010*, Prog. Theor. Phys. Suppl. **187**, 17 (2011), arXiv:1011.3204 [hep-ph]
- [41] Y. I. Azimov, Y. L. Dokshitzer, V. A. Khoze, and S. I. Troyan, Z. Phys. **C27**, 65 (1985)
- [42] K. J. Golec-Biernat and M. Wusthoff, Phys. Rev. **D59**, 014017 (1998), arXiv:hep-ph/9807513 [hep-ph]
- [43] S. Acharya *et al.* (ALICE), Phys. Rev. **C99**, 024906 (2019), arXiv:1807.11321 [nucl-ex]
- [44] B. B. Abelev *et al.* (ALICE), Phys. Lett. **B728**, 25 (2014), arXiv:1307.6796 [nucl-ex]
- [45] S. Chatrchyan *et al.* (CMS), Eur. Phys. J. **C72**, 2164 (2012), arXiv:1207.4724 [hep-ex]
- [46] A. M. Sirunyan *et al.* (CMS), Phys. Rev. **D96**, 112003 (2017), arXiv:1706.10194 [hep-ex]
- [47] S. Chatrchyan *et al.* (CMS), Eur. Phys. J. **C74**, 2847 (2014), arXiv:1307.3442 [hep-ex]
- [48] J. Adam *et al.* (ALICE), Phys. Lett. **B760**, 720 (2016), arXiv:1601.03658 [nucl-ex]
- [49] M. A. Lisa, S. Pratt, R. Soltz, and U. Wiedemann, Ann. Rev. Nucl. Part. Sci. **55**, 357 (2005), arXiv:nucl-ex/0505014
- [50] K. Aamodt *et al.* (ALICE), Phys. Rev. D **84**, 112004 (2011), arXiv:1101.3665 [hep-ex]
- [51] V. Khachatryan *et al.* (CMS), JHEP **05**, 029 (2011), arXiv:1101.3518 [hep-ex]
- [52] S. Acharya *et al.* (ALICE), Eur. Phys. J. **C79**, 857 (2019), arXiv:1905.07208 [nucl-ex]
- [53] K. Itakura, *New frontiers in QCD: Fundamental problems in hot and/or dense matter. Proceedings, International Workshop and Symposium, YIPQS, Kyoto, Japan, March 3-6, 2008*, Prog. Theor. Phys. Suppl. **174**, 181 (2008)
- [54] C. Andres, A. Moscoso, and C. Pajares, Nucl. Phys. A **901**, 14 (2013), arXiv:1212.3102 [nucl-th]
- [55] The experimental data for nuclear modification factors are obtained using inclusive transverse momentum spectra, including various multiplicities events. Therefore, it is necessary to compare the data on the nuclear correction factors using semi-inclusive events with our model for a more accurate discussion.
- [56] S. Acharya *et al.* (ALICE), Phys. Rev. C **101**, 044907 (2020), arXiv:1910.07678 [nucl-ex]
- [57] B. Abelev *et al.* (ALICE), Phys. Rev. Lett. **110**, 032301 (2013), arXiv:1210.3615 [nucl-ex]
- [58] M. Aaboud *et al.* (ATLAS), Phys. Lett. B **796**, 230 (2019), arXiv:1903.02209 [nucl-ex]
- [59] J. Dias de Deus and C. Pajares, Phys. Lett. B **695**, 211 (2011), arXiv:1011.1099 [hep-ph]
- [60] M. Braun and C. Pajares, Phys. Rev. Lett. **85**, 4864 (2000), arXiv:hep-ph/0007201
- [61] M. Braun, F. Del Moral, and C. Pajares, Phys. Rev. C **65**, 024907 (2002), arXiv:hep-ph/0105263
- [62] M. Braun and C. Pajares, Eur. Phys. J. C **16**, 349 (2000), arXiv:hep-ph/9907332
- [63] W. Zhang and C. Yang, J. Phys. G **41**, 105006 (2014), arXiv:1403.5347 [hep-ph]